

Simple Finite Element Methods for Approximating Predator–Prey Dynamics in Two Dimensions Using Matlab

Marcus R. Garvie, John Burkardt & Jeff Morgan

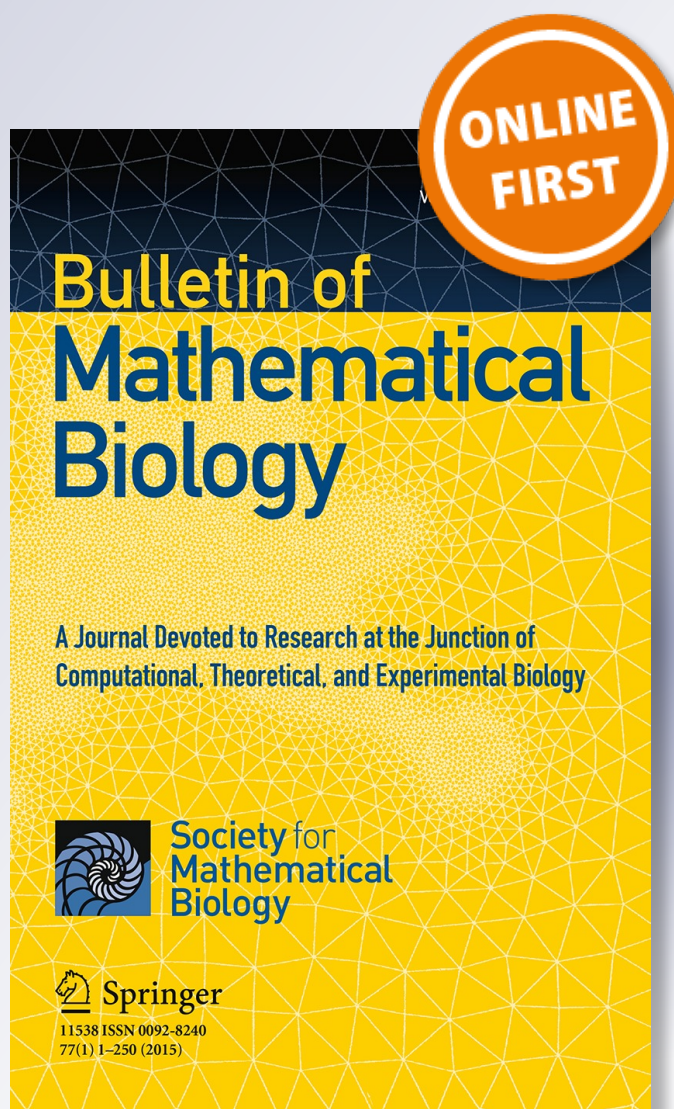
Bulletin of Mathematical Biology

A Journal Devoted to Research at the Junction of Computational, Theoretical and Experimental Biology Official Journal of The Society for Mathematical Biology

ISSN 0092-8240

Bull Math Biol

DOI 10.1007/s11538-015-0062-z



Your article is protected by copyright and all rights are held exclusively by Society for Mathematical Biology. This e-offprint is for personal use only and shall not be self-archived in electronic repositories. If you wish to self-archive your article, please use the accepted manuscript version for posting on your own website. You may further deposit the accepted manuscript version in any repository, provided it is only made publicly available 12 months after official publication or later and provided acknowledgement is given to the original source of publication and a link is inserted to the published article on Springer's website. The link must be accompanied by the following text: "The final publication is available at link.springer.com".

Simple Finite Element Methods for Approximating Predator–Prey Dynamics in Two Dimensions Using MATLAB

Marcus R. Garvie · John Burkardt · Jeff Morgan

Received: 9 June 2014 / Accepted: 5 January 2015
© Society for Mathematical Biology 2015

Abstract We describe simple finite element schemes for approximating spatially extended predator–prey dynamics with the Holling type II functional response and logistic growth of the prey. The finite element schemes generalize ‘Scheme 1’ in the paper by Garvie (Bull Math Biol 69(3):931–956, 2007). We present user-friendly, open-source MATLAB code for implementing the finite element methods on arbitrary-shaped two-dimensional domains with Dirichlet, Neumann, Robin, mixed Robin–Neumann, mixed Dirichlet–Neumann, and Periodic boundary conditions. Users can download, edit, and run the codes from <http://www.uoguelph.ca/~mgarvie/>. In addition to discussing the well posedness of the model equations, the results of numerical experiments are presented and demonstrate the crucial role that habitat shape, initial data, and the boundary conditions play in determining the spatiotemporal dynamics of predator–prey interactions. As most previous works on this problem have focussed on square domains with standard boundary conditions, our paper makes a significant contribution to the area.

Keywords Predator–prey · Reaction–diffusion · Complex geometry · Mixed boundary conditions · Well posed · Finite element method · MATLAB

M. R. Garvie (✉)

Department of Mathematics and Statistics, University of Guelph, Guelph, ON N1G 2W1, Canada
e-mail: mgarvie@uoguelph.ca

J. Burkardt

Department of Scientific Computing, Florida State University, Tallahassee, FL 32306-4120, USA
e-mail: jburkardt@fsu.edu

J. Morgan

Department of Mathematics, The University of Houston, Houston, TX 77204-3008, USA
e-mail: jmorgan@math.uh.edu

1 Introduction

1.1 Background

Complicated geometrical shapes occur throughout the natural world and have an important role to play in determining the behaviour of complex systems and pattern formation phenomena. For example, tumour growth in humans (Friedman 2012; Chaplain et al. 2001), the development of coat patterns in mammals (Murray 1981; Bassiri et al. 2009), cardiac arrhythmia (Holden et al. 1991; Bittihn et al. 2010), and predator–prey interactions in bounded domains (Gurney et al. 1998; Medvinsky et al. 2002) all depend on the geometry of the physical situation where these phenomena take place.

In this paper, we study the numerical solutions of parabolic partial differential equations (PDEs) defined on arbitrary-shaped two-dimensional domains with various boundary and initial conditions. We focus on finite element approximations of a well-known reaction–diffusion system for predator–prey interactions. As a minimum, we expect readers of this paper to have taken prerequisite courses in PDEs and matrix algebra.

Reaction–diffusion equations are a useful tool for modelling the spatiotemporal dynamics of populations in ecology (Cantrell and Cosner 2003; Holmes et al. 1994), and their use in the biological sciences continues to receive intense interest because of their many applications (Murray 2002, 2003). Modelling with reaction–diffusion equations is motivated by an increasing awareness of the role that space has on population dynamics. Furthermore, advances in mathematical modelling coupled with an increase in the computational power of microcomputers make it easier to study more realistic problems.

The finite element method is an effective and powerful numerical method for solving nonlinear PDEs and is particularly well suited to problems defined on irregular-shaped domains (Ciarlet 1979). The success of the finite element method is also due to the well-established theoretical framework for numerical analysis (Strang and Fix 1973; Thomée 2006; Brenner and Scott 1994).

It is important to consider spatial heterogeneity when investigating the basic ecological features of a habitat, such as invasion, critical patch size, spatial spread, persistence, and the spatiotemporal dynamics of populations (Tilman and Kareiva 1997; Cantrell and Cosner 2003; Holmes et al. 1994). Furthermore, the rules governing how species behave near habitat edges (incorporated as the boundary conditions in PDEs) have important implications for these ecological (population level) characteristics (Maciel and Lutscher 2013; Fagan et al. 1999). However, most theoretical and numerical PDE studies of spatially extended predator–prey interactions are either in one space dimension, or in two space dimensions on square domains with either the homogeneous Neumann ('zero flux'), or homogeneous Dirichlet boundary conditions; see, for example Medvinsky et al. 2002; Garvie 2007; Gurney et al. 1998.

There are some notable exceptions to the sparsity of spatially extended predator–prey studies with nonstandard boundary conditions and/or irregular-shaped domains. For instance, Sherratt (2003) investigated the generation of periodic travelling waves for the lambda–omega reaction–diffusion system in two space dimensions on an irreg-

ular domain using homogeneous Dirichlet boundary conditions. Similar studies incorporate homogeneous Dirichlet boundary conditions on the boundary of irregular landscape obstacles, which generate periodic travelling waves for oscillatory reaction–diffusion equations (Sherratt et al. 2002, 2003; Sherratt and Smith 2008; Smith et al. 2008; Yun et al. 2011). In a rare computational study, Ding and Kawahara (1998) computed the travelling wave solutions of the spatially extended Lotka–Volterra system for a shallow bay in Japan. The authors compared the results from a three-step explicit finite element method with a superposition method using normal modes. With regard to the use of nonstandard boundary conditions in two dimensions, researchers have also studied: Periodic boundary conditions (Malchow et al. 2004; Hilker et al. 2006), mixed Periodic–Neumann boundary conditions (Malchow et al. 2000, 2002), and mixed Neumann–Dirichlet boundary conditions (Smith et al. 2009; Sherratt and Smith 2008). Sherratt (2008) compared periodic wave generation for oscillatory reaction–diffusion systems with both the Robin and the Dirichlet boundary conditions. Another important paper by Cantrell et al. (1998) studied a coupled pair of diffusive Lotka–Volterra competition equations with Robin boundary conditions in two or three space dimensions. The authors investigated how the boundary conditions affect the outcome of competitive interactions between the species. We also mention a paper by Kaipio et al. (1995) that used the finite element method to approximate the solutions of a predator–prey model over a circular domain with homogeneous Dirichlet boundary conditions. Theoretical studies include: an existence–uniqueness work by Shanger-ganesh and Balachandran (2011) for a predator–prey model on a three-dimensional habitat with mixed Neumann–Dirichlet boundary conditions, and a study in arbitrary space dimensions of a model that includes the Lotka–Volterra model with nonlinear (mixed) coupled boundary conditions (Leung 1982).

1.2 Model Equations

We study a reaction–diffusion system for spatially extended predator–prey interactions with the following nondimensional (classical) form:¹

$$\boxed{\text{prey}} \quad \frac{\partial u}{\partial t} = \overbrace{\Delta u}^{\text{dispersal}} + \overbrace{u(1-u)}^{\text{intrinsic birth and death}} - \overbrace{\frac{uv}{u+\alpha}}^{\text{predation}}, \tag{1a}$$

$$\boxed{\text{predators}} \quad \frac{\partial v}{\partial t} = \overbrace{\delta \Delta v}^{\text{dispersal}} + \overbrace{\frac{\beta uv}{u+\alpha}}^{\text{benefit from predation}} - \overbrace{\gamma v}^{\text{death}}, \tag{1b}$$

where $u(\mathbf{x}, t)$ and $v(\mathbf{x}, t)$ are the population densities of prey and predators at time t and (vector) position $\mathbf{x} := (x, y)^T \in \mathbb{R}^2$. We use the usual Laplacian operator $\Delta \equiv \frac{\partial^2}{\partial x^2} + \frac{\partial^2}{\partial y^2}$ in two space dimensions, and the parameters $\alpha, \delta, \beta,$ and γ are strictly positive. We assume system (1) is defined over a bounded domain $\Omega \subset \mathbb{R}^2$ with a

¹ See the paper by Garvie and Trenchea (2010) for details of the nondimensionalization procedure.

smooth, or Lipschitz polygonal boundary Γ . The domain is either simply connected, or multiply connected (contains holes). Multiply connected regions are useful for modelling species living in fragmented landscapes, for example, phytoplankton and zooplankton in lakes containing islands, or species living in a forest containing pockets of grassland. To complete the partial differential equation (PDE) model (1), we require appropriate nonnegative initial conditions

$$u(\mathbf{x}, 0) := u_0(\mathbf{x}), \quad v(\mathbf{x}, 0) := v_0(\mathbf{x}), \quad \text{for all } \mathbf{x} \text{ in } \Omega, \quad (2)$$

and boundary conditions. The boundary conditions considered in this paper are fairly general, namely Neumann, Dirichlet, Robin, and Periodic boundary conditions. We also consider the case of mixed Dirichlet–Neumann and mixed Robin–Neumann boundary conditions (see Sect. 2.1 below for full details).

In the above model, the reaction kinetics have the classic Rosenzweig–MacArthur form, i.e. the local growth of the prey is logistic and the predator displays the ‘Holling type II functional response’ (Holling 1959). For details concerning the derivation of Holling’s functional responses in predator–prey systems, see the paper by Dawes and Souza (2013). The labelling of the different terms in (1) follows Sherratt et al. 2003; Sherratt 2008. This system is arguably the most well-known reasonably realistic (minimal) PDE model for predator–prey dynamics (May 1974; Sherratt 2001; Garvie 2007; Garvie and Trenchea 2007).

Although the dynamics of the reaction–diffusion system are more complicated than the reduced (diffusionless) system, a consideration of the local dynamics provides important guidelines for choosing biologically relevant parameters when numerically solving the full reaction–diffusion system (Medvinsky et al. 2002). The local dynamics of system (1) are well understood (Garvie 2007; Medvinsky et al. 2002; Malchow and Petrovskii 2002); however, for convenience, we summarize the main features below.

Firstly, it follows from a consideration of the nullclines of the system that if the initial data are chosen in the (biologically relevant) nonnegative orthant, then $u \geq 0, v \geq 0$ for all time. This is also true for the full reaction–diffusion system, which follows from the invariant region theory of Smoller (1983). From linear stability analysis, it follows that the reduced system has three possible stationary points, namely (0, 0) (extinction), (1, 0) (predator extinction), and (u^*, v^*) corresponding to the coexistence of prey and predators, where

$$u^* = \frac{\alpha\gamma}{\beta - \gamma}, \quad v^* = (1 - u^*)(u^* + \alpha). \quad (3)$$

It follows immediately from (3) that in order for the stationary states to be in the positive orthant we must have $u^* < 1, \beta > \gamma$, which implies $\alpha < (\beta - \gamma)/\gamma$. We are mainly interested in the case when the reaction kinetics possess a stable limit cycle surrounding the unstable stationary point (u^*, v^*) , i.e. the predators and prey are oscillatory, which occurs when Garvie and Trenchea (2010):

$$\alpha < \frac{\beta - \gamma}{\beta + \gamma}, \quad (\beta > \gamma). \quad (4)$$

The main focus of this paper is on the spatiotemporal dynamics of the full (spatially structured) reaction–diffusion system. Although the predator–prey system (1) is a minimal model in the sense that only a few key interactions are taken into account, the system displays a wide range of ecologically relevant behaviour, for example, spiral waves (Medvinsky et al. 2002), target waves (Sherratt et al. 1997), and spatiotemporal ‘chaos’ (Pascual 1993; Medvinsky et al. 2002). However, diffusion-induced instability is not possible for this particular model (Malchow et al. 2008, p. 212), (Segel and Jackson 1972; Peacock-Lopez 2011).

1.3 Aims

Our paper generalizes some finite element methods by Garvie (2007) (see also Alberty et al. 1999) for predator–prey dynamics on square domains with the homogeneous Neumann boundary conditions. The main aims of our work are as follows:

- (i) To completely describe the construction of finite element methods for approximating system (1) defined over arbitrary-shaped domains in two space dimensions with various boundary conditions (see Sect. 2.1). The methods generalize ‘Scheme 1’ for ‘Kinetics (i)’ in the paper by Garvie (2007).
- (ii) To provide and briefly describe user-friendly, open-source MATLAB codes, available at <http://www.uoguelph.ca/~mgarvie/>, for implementing the finite element methods. The MATLAB codes for the generalization of ‘Scheme 2’ in Garvie (2007) are also provided, but due to space constraints are not described.
- (iii) To provide a number of ecologically relevant examples demonstrating the crucial role that habitat shape, boundary conditions, and initial conditions play in determining the spatiotemporal dynamics of predator–prey dynamics.
- (iv) To facilitate the numerical study of the spatiotemporal dynamics of predator–prey interactions, without requiring an advanced knowledge of PDEs or programming.

Although we focus on a specific predator–prey system, the methodology in our paper has general applicability to many other reaction–diffusion systems. For further details, see the mathematical biology texts by Murray (2003), Meinhardt (1982), Malchow et al. (2008), Edelstein-Keshet (2005), and the models therein.

1.4 Structure of the Paper

In Sect. 2, we describe the different boundary conditions employed, present the variational formulations of the predator–prey systems, and give an outline of a proof for the well posedness of the classical predator–prey systems. In Sect. 3, we present the fully discrete finite element methods for approximating the predator–prey models, derive the resulting linear systems of equations to be solved at each time step, and give a description of the MATLAB code that implements the finite element methods. In Sect. 4, we present the results of some numerical experiments using MATLAB, while in Sect. 5, we make some concluding comments from both a numerical and an ecological perspective.

2 Mathematical Preliminaries

2.1 Boundary Conditions

The pure Neumann, Dirichlet, and Robin boundary conditions for the predator–prey system (1) have the following forms, where n is the unit outward normal vector to the boundary Γ of the domain Ω :

$$\text{Neumann:} \quad \frac{\partial u}{\partial n} = g_u(\mathbf{x}, t), \quad \delta \frac{\partial v}{\partial n} = g_v(\mathbf{x}, t) \text{ on } \Gamma, \quad (5)$$

$$\text{Dirichlet:} \quad u = f_u(\mathbf{x}, t), \quad v = f_v(\mathbf{x}, t) \text{ on } \Gamma, \quad (6)$$

$$\text{Robin:} \quad \frac{\partial u}{\partial n} = k_1 u, \quad \delta \frac{\partial v}{\partial n} = k_2 v, \quad \text{on } \Gamma. \quad (7)$$

The functions $g_u(\mathbf{x}, t)$, $g_v(\mathbf{x}, t)$, $f_u(\mathbf{x}, t)$, and $f_v(\mathbf{x}, t)$ are arbitrary nonnegative functions of space and time² and k_1 and k_2 are constants. When $g_u = g_v = 0$, we have the homogeneous Neumann (‘zero flux’) boundary conditions, which correspond to the ecological situation of species neither entering nor leaving the domain. However, when $f_u = f_v = 0$, we have the homogeneous Dirichlet boundary conditions corresponding to a lethal boundary, or when all individuals at the boundary leave Ω and do not return (Sherratt et al. 2003; Cantrell and Cosner 2003; Maciel and Lutscher 2013; Fagan et al. 1999).

The homogeneous Neumann and homogeneous Dirichlet boundary conditions are frequently used for computational and mathematical convenience. However, the choice of boundary conditions should be dictated by modelling concerns. For example, if we wish to model the use of nonlethal fencing as a conservation tool to exclude certain predators from a habitat (see Malpas et al. 2013), then the homogeneous Neumann boundary condition is appropriate. On the other hand, if a lethal electrified fence is used to exclude pests from a habitat (see Ahmed and Fiedler 2002), then the homogeneous Dirichlet boundary condition is a more natural choice.

The Robin boundary conditions correspond to when species enter ($k > 0$), or leave ($k < 0$) the domain Ω across the boundary Γ . In ecological situations, a Robin boundary condition of this type may be more realistic than the frequently used homogeneous Dirichlet boundary condition (Sherratt 2008; Maciel and Lutscher 2013). When $k = 0$, the condition says that there is no flux across Γ ; however, as k increases in magnitude, a larger number of individuals will cross the boundary. In the limit as $k \rightarrow -\infty$, the condition becomes the homogeneous Dirichlet boundary condition (Cantrell and Cosner 2003). (The case $k \rightarrow +\infty$ leads to ‘blow-up’.) Thus, we have a range of Robin boundary conditions with the homogeneous Neumann and the homogeneous Dirichlet boundary conditions representing the extreme ends of this range.

We are also interested in Periodic boundary conditions on the square $[a, b] \times [a, b]$ ($a, b \in \mathbb{R}$), which have the following form for $w \equiv w(x, y, t)$ ($w = u$ or v):

² The requirement $g_u > 0$, $g_v > 0$ is necessary to avoid possible (nonphysical) negative solutions as $t \rightarrow \infty$.

Periodic: $w(a, y, t) = w(b, y, t)$ for all $a \leq y \leq b$, (8a)

$$w_x(a, y, t) = w_x(b, y, t) \quad \text{for all } a \leq y \leq b, \quad (8b)$$

$$w(x, a, t) = w(x, b, t) \quad \text{for all } a \leq x \leq b. \quad (8c)$$

$$w_y(x, a, t) = w_y(x, b, t) \quad \text{for all } a \leq x \leq b. \quad (8d)$$

Periodic boundary conditions are useful for modelling situations formulated on large, or effectively unbounded domains, where we want to minimize boundary effects on the solutions. For example, periodic boundary conditions are appropriate for models of the patchy distribution of plankton in the ocean (Malchow et al. 2004; Hilker et al. 2006), where the boundary is needed simply for computational reasons. Periodic boundary conditions are also used because of the ease with which they are implemented in numerical simulations (Descalzi and Brand 2008).

In practice, due to the complex heterogeneity of natural landscapes, the real world can be modelled as a network of patches with mixed boundary conditions. An example of such a habitat might be deer living in patches of forest connected by migration, with arable land surrounding the patches (a metapopulation). To model this situation, the Robin boundary condition is a reasonable choice to impose on the boundary of the patches (see the paper by Cantrell et al. 1998). However, if there are landscape obstacles that block animal movement (e.g. a fence), then the mixed Robin–Neumann boundary condition might be more appropriate. Alternatively, if the patches are intersected by a highway lethal to animal movement, then the mixed Robin–Dirichlet boundary condition might be a better choice. It is not difficult to conceive of other mixed boundary condition scenarios depending on the particular landscape heterogeneity involved. Thus, in addition to the four (pure) boundary conditions defined above, we also consider two mixed boundary conditions. We assume the boundary Γ contains two relatively open subsets Γ_1 and Γ_2 where

$$\Gamma := \overline{\Gamma_1} \cup \overline{\Gamma_2}, \quad \Gamma_1 \cap \Gamma_2 = \emptyset.$$

Then, the mixed boundary conditions are defined as follows:

Mixed Robin–Neumann:

$$\frac{\partial u}{\partial n} = k_1 u, \quad \delta \frac{\partial v}{\partial n} = k_2 v \quad \text{on } \Gamma_1, \quad (9a)$$

$$\frac{\partial u}{\partial n} = g_u(\mathbf{x}, t), \quad \delta \frac{\partial v}{\partial n} = g_v(\mathbf{x}, t) \quad \text{on } \Gamma_2. \quad (9b)$$

Mixed Dirichlet–Neumann:

$$u = f_u(\mathbf{x}, t), \quad v = f_v(\mathbf{x}, t) \quad \text{on } \Gamma_1, \quad (10a)$$

$$\frac{\partial u}{\partial n} = g_u(\mathbf{x}, t), \quad \delta \frac{\partial v}{\partial n} = g_v(\mathbf{x}, t) \quad \text{on } \Gamma_2. \quad (10b)$$

If $\Gamma_1 = \emptyset$ in either mixed case, we have pure Neumann boundary conditions, while if $\Gamma_2 = \emptyset$ in the first or second mixed boundary condition case, then we have the pure Robin or Dirichlet boundary conditions, respectively.

2.2 Variational ('Weak') Formulations

The starting point for constructing the finite element approximations of the predator–prey system is the variational (or weak) formulation of the problem. In order to reformulate the problem in variational form, the type of boundary conditions plays an important role. However, before we state the variational formulations, we need to briefly mention some abstract function spaces needed in the sequel [for a more complete treatment of these spaces, see Grossmann et al. 2007; Larsson and Thomée 2009; Adams 1975]. The basic underlying space is the set of square integrable functions $L^2(\Omega)$, where Ω is a bounded domain in \mathbb{R}^2 , given by

$$L^2(\Omega) := \left\{ v : v \text{ defined on } \Omega \text{ such that } \int_{\Omega} |v|^2 \, d\mathbf{x} < \infty \right\},$$

which is a Hilbert space with respect to the inner product

$$(v, w) := \int_{\Omega} v(\mathbf{x})w(\mathbf{x}) \, d\mathbf{x},$$

(here $d\mathbf{x} := dx \, dy$). We also require the L^2 inner product over the boundary Γ (or a piece of the boundary)

$$(v, w)_{\Gamma} := \int_{\Gamma} v(\mathbf{x})w(\mathbf{x}) \, ds,$$

where ds is an element of arc length for functions in $L^2(\Gamma)$. The following Hilbert space is standard:

$$H^1(\Omega) := \left\{ v \in L^2(\Omega) : \frac{\partial v}{\partial x}, \frac{\partial v}{\partial y} \in L^2(\Omega) \right\}. \tag{11}$$

We are now in a position to state the variational formulations of the predator–prey system (1) with the initial conditions (2) and the boundary conditions given by (8), (9), or (10). In each case, this is derived formally by multiplying the PDEs in (1) by an appropriate test function η (in either $H^1(\Omega)$ or a subspace thereof), integrating over the domain Ω and applying the usual Green's formula

$$\int_{\Omega} \nabla u \cdot \nabla v \, d\mathbf{x} = \int_{\Gamma} \frac{\partial u}{\partial n} v \, ds - \int_{\Omega} v \Delta u \, d\mathbf{x},$$

[e.g. (Larsson and Thomée 2009, p. 5)]. To simplify the notation, we define the reaction kinetics for the predators and prey in (1) by

$$h_1(u, v) := u(1 - u) - \frac{uv}{u + \alpha}, \quad h_2(u, v) := \frac{\beta uv}{u + \alpha} - \gamma v. \tag{12}$$

Then, the variational formulations covering all possible pure or mixed boundary condition cases can be expressed in just three problems. The problem with mixed Robin–Neumann boundary conditions has the form:

Weak Problem I: Given initial data $u_0(\cdot), v_0(\cdot)$, seek $u(\cdot, t), v(\cdot, t) \in H^1(\Omega)$, $t > 0$, satisfying

$$(u_t, \eta) + (\nabla u, \nabla \eta) = k_1(u, \eta)_{\Gamma_1} + (g_u, \eta)_{\Gamma_2} + (h_1, \eta), \quad \forall \eta \in H^1(\Omega), \quad (13a)$$

$$(v_t, \eta) + \delta(\nabla v, \nabla \eta) = k_2(v, \eta)_{\Gamma_1} + (g_v, \eta)_{\Gamma_2} + (h_2, \eta), \quad \forall \eta \in H^1(\Omega). \quad (13b)$$

If we let $\Gamma_1 = \emptyset$, then we have the pure Neumann problem, while if we let $\Gamma_2 = \emptyset$, then we have the pure Robin problem. The Neumann and Robin boundary conditions are imposed implicitly through the incorporation of boundary terms into the weak formulation.

The weak formulation with mixed Dirichlet–Neumann boundary conditions (Grossmann et al. 2007; Barrett and Elliott 1986) has the form:

Weak Problem II: Given initial data $u_0(\cdot), v_0(\cdot)$, seek $u(\cdot, t) \in H^1_{E_u}(\Omega)$ and $v(\cdot, t) \in H^1_{E_v}(\Omega)$, $t > 0$, satisfying

$$(u_t, \eta) + (\nabla u, \nabla \eta) = (g_u, \eta)_{\Gamma_2} + (h_1, \eta), \quad \forall \eta \in H^1_0(\Omega; \Gamma_1), \quad (14a)$$

$$(v_t, \eta) + \delta(\nabla v, \nabla \eta) = (g_v, \eta)_{\Gamma_2} + (h_2, \eta), \quad \forall \eta \in H^1_0(\Omega; \Gamma_1), \quad (14b)$$

where

$$H^1_{E_u}(\Omega) := \left\{ w \in H^1(\Omega) : w = f_u(\mathbf{x}, t) \text{ on } \Gamma_1 \right\}, \quad (15a)$$

$$H^1_{E_v}(\Omega) := \left\{ w \in H^1(\Omega) : w = f_v(\mathbf{x}, t) \text{ on } \Gamma_1 \right\}, \quad (15b)$$

$$H^1_0(\Omega; \Gamma_1) := \left\{ w \in H^1(\Omega) : w = 0 \text{ on } \Gamma_1 \right\}. \quad (15c)$$

If we let $\Gamma_2 = \emptyset$, then we have the pure Dirichlet problem. The Dirichlet boundary conditions must be imposed explicitly on the trial (solution) space. Finally, we give a weak formulation of the Periodic problem (Temam 1997, pp. 66–67):

Weak Problem III: With $\Omega := [a, b]^2$ and given initial data $u_0(\cdot), v_0(\cdot)$, seek $u(\cdot, t), v(\cdot, t)$ in $H^1_{\text{per}}(\Omega)$, $t > 0$, satisfying

$$(u_t, \eta) + (\nabla u, \nabla \eta) = (h_1, \eta), \quad \forall \eta \in H^1_{\text{per}}(\Omega), \quad (16a)$$

$$(v_t, \eta) + \delta(\nabla v, \nabla \eta) = (h_2, \eta), \quad \forall \eta \in H^1_{\text{per}}(\Omega), \quad (16b)$$

where

$$H^1_{\text{per}}(\Omega) := \left\{ w \in H^1(\Omega) : w(a, y) = w(b, y), w(x, a) = w(x, b), \forall x, y \in [a, b] \right\}. \quad (17)$$

Note that conditions (8b) and (8d) are naturally incorporated in the weak formulation [see Temam (1997, pp. 66–67) for a mathematical justification]. However, the boundary conditions for the periodicity of the solutions are imposed explicitly on the trial (solution) space.

2.3 Well Posedness of the Predator–Prey Problem

Throughout we assume $u_0, v_0 \in H^2(\Omega)$ are nonnegative, and g_u, g_v, f_u and f_v are nonnegative smooth-bounded functions on $\partial\Omega \times [0, T]$ for each $T > 0$. It is possible to obtain uniqueness and well-posedness results with lesser hypotheses, but we wish to keep the discussion as simple as possible and illustrate the main ideas. Additional hypotheses must be imposed on u_0 and v_0 depending on the boundary conditions. In the case of Problem I, we assume

$$\frac{\partial u_0}{\partial n} = k_1 u_0, \delta \frac{\partial v_0}{\partial n} = k_2 v_0 \text{ on } \Gamma_1 \text{ and } \frac{\partial u_0}{\partial n} = g_u |_{t=0}, \delta \frac{\partial v_0}{\partial n} = g_v |_{t=0} \text{ on } \Gamma_2.$$

In the case of Problem II, we assume

$$u_0 = f_u |_{t=0}, v_0 = f_v |_{t=0} \text{ on } \Gamma_1 \text{ and } \frac{\partial u_0}{\partial n} = g_u |_{t=0}, \delta \frac{\partial v_0}{\partial n} = g_v |_{t=0} \text{ on } \Gamma_2.$$

In the case of Problem III, we assume $u_0, v_0, \frac{\partial u_0}{\partial n}, \frac{\partial v_0}{\partial n} \in H^1_{\text{per}}(\Omega)$. If $T > 0$, then the spaces $L^2(\Omega \times (0, T))$ and $W^{1,1}(\Omega \times (0, T))$ are defined analogously to $L^2(\Omega)$ and $H^1(\Omega)$ in Sect. 2.2, and

$$\begin{aligned} \overset{\circ}{W}^{1,1}(\Omega \times (0, T)) &= \{w \in W^{1,1}(\Omega \times (0, T)) : w(\cdot, T) = 0\}, \\ W_{\circ}^{1,1}(\Omega \times (0, T); \Gamma_1) &= \{w \in W^{1,1}(\Omega \times (0, T)) : w(\cdot, t) |_{\Gamma_1} = 0 \text{ a.e. } 0 < t < T\}, \\ \overset{\circ}{W}^{1,1}(\Omega \times (0, T); \Gamma_1) &= \overset{\circ}{W}^{1,1}(\Omega \times (0, T)) \cap W_{\circ}^{1,1}(\Omega \times (0, T); \Gamma_1), \\ W_{\text{per}}^{1,1}(\Omega \times (0, T)) &= \{w \in W^{1,1}(\Omega \times (0, T)) : w(\cdot, t) \in H^1_{\text{per}}(\Omega) \text{ a.e. } 0 < t < T\}, \\ \overset{\circ}{W}^{1,1}_{\text{per}}(\Omega \times (0, T)) &= W_{\text{per}}^{1,1}(\Omega \times (0, T)) \cap \overset{\circ}{W}^{1,1}(\Omega \times (0, T)). \end{aligned}$$

We give precise notions of solvability for Problems I, II, and III below.

Definition 2.1 We say $u, v \in W^{1,1}(\Omega \times (0, T))$ is a solution of Problem I for $0 < t < T$ if and only if for all $\gamma \in \overset{\circ}{W}^{1,1}(\Omega \times (0, T))$

$$\begin{aligned} \int_0^T (-u, \gamma_t) + (\nabla u, \nabla \gamma) dt &= \int_0^T (k_1(u, \gamma)_{\Gamma_1} + (g_u, \gamma)_{\Gamma_2} dt + (u_0, \gamma(\cdot, 0)), \\ \int_0^T (-v, \gamma_t) + \delta(\nabla v, \nabla \gamma) dt &= \int_0^T (k_2(v, \gamma)_{\Gamma_1} + (g_v, \gamma)_{\Gamma_2} dt + (v_0, \gamma(\cdot, 0)). \end{aligned}$$

Definition 2.2 We say $u, v \in W^{1,1}(\Omega \times (0, T))$ is a solution of Problem II for $0 < t < T$ if and only if $u = f_u$ and $v = g_v$ on $\Gamma_1 \times (0, T)$ and for all $\gamma \in \overset{\circ}{W}^{1,1}(\Omega \times (0, T); \Gamma_1)$

$$\int_0^T (-u_t, \gamma_t) + (\nabla u, \nabla \gamma) dt = \int_0^T ((g_u, \gamma)_{\Gamma_2} + (h_1, \gamma)) dt + (u_0, \gamma(\cdot, 0)),$$

$$\int_0^T (-v_t, \gamma_t) + \delta(\nabla v, \nabla \gamma) dt = \int_0^T ((g_v, \gamma)_{\Gamma_2} + (h_2, \gamma)) dt + (v_0, \gamma(\cdot, 0)).$$

Definition 2.3 We say $u, v \in W_{\text{per}}^{1,1}(\Omega \times (0, T))$ is a solution of Problem III for $0 < t < T$ if and only if for all $\gamma \in \overset{\circ}{W}_{\text{per}}^{1,1}(\Omega \times (0, T))$

$$\int_0^T (-u_t, \gamma_t) + (\nabla u, \nabla \gamma) dt = \int_0^T ((h_1, \gamma)) dt + (u_0, \gamma(\cdot, 0)),$$

$$\int_0^T (-v_t, \gamma_t) + \delta(\nabla v, \nabla \gamma) dt = \int_0^T ((h_2, \gamma)) dt + (v_0, \gamma(\cdot, 0)).$$

It is straightforward to prove that functions, which solve Problems I, II, and III according to the definitions above, also satisfy the weak formulations of these problems stated in Sect. 2.2. We say that the problems defined above have global solutions if and only if there are functions u, v so that for every $T > 0$, u, v are solutions for $0 < t < T$.

Theorem 2.4 *Problems I, II, and III have unique, nonnegative, global solutions. Furthermore, there is a function $\varphi \in C([0, \infty))$ such that $0 \leq u(\mathbf{x}, t), v(\mathbf{x}, t) \leq \varphi(t)$ for all $t \geq 0$.*

If the functions f_u, f_v, g_u , and g_v are uniformly bounded and $k_1, k_2 < 0$, then it is possible to show that the solutions are uniformly bounded. We outline the main idea of the proof for Problem III below. The proofs in the other cases are similar.

Proof (outline) Let $T, R > 0$ and define $\mathbb{R}_+ = [0, \infty)$, and for $z \in \mathbb{R}, z_+ = \begin{cases} z, & z \geq 0, \\ 0, & z < 0 \end{cases}$ and $z_- = (-z)_+$. Let $\phi_R \in C^\infty(\mathbb{R}_+, [0, 1])$ such that $\phi_R(z) = 1$ if $0 \leq z \leq R$ and $\phi(z) = 0$ if $z \geq 2R$. Define

$$h_{1,R}(u, v) = \phi_R(u_+)h_1(u_+, v_+), \quad h_{2,R}(u, v) = \phi_R(u_+)h_2(u_+, v_+),$$

and $\mathcal{L}_R : L^2(\Omega \times (0, T), \mathbb{R}^2) \rightarrow L^2(\Omega \times (0, T), \mathbb{R}^2)$ by $\mathcal{L}_R(\tilde{u}, \tilde{v}) = (u, v)$ where $u, v \in W_{\text{per}}^{1,1}(\Omega \times (0, T))$ are the unique solutions to

$$\int_0^T (-u_t, \gamma_t) + (\nabla u, \nabla \gamma) dt = \int_0^T ((h_{1,R}(\tilde{u}_+, \tilde{v}_+), \gamma)) dt + (u_0, \gamma(\cdot, 0)), \quad (18a)$$

$$\int_0^T (-v_t, \gamma_t) + \delta(\nabla v, \nabla \gamma) dt = \int_0^T ((h_{2,R}(\tilde{u}_+, \tilde{v}_+), \gamma)) dt + (v_0, \gamma(\cdot, 0)). \quad (18b)$$

for all $\gamma \in \overset{\circ}{W}_{\text{per}}^{1,1}(\Omega \times (0, T))$. Straightforward adaptations of the arguments in Chapter 3 of the book by Ladyženskaja et al. (1968) guarantee that \mathcal{L}_R is well defined since $h_{i,R}(\tilde{u}, \tilde{v}) \in L^2(\Omega \times (0, T))$ for all $\tilde{u}, \tilde{v} \in L^2(\Omega \times (0, T))$. Furthermore, it is a

simple matter to show that \mathcal{L}_R has a fixed point if we can demonstrate that there exists $L_T \geq 0$ so that whenever $0 \leq \lambda \leq 1$ and $u, v \in L^2(\Omega \times (0, T))$ then

$$\|u\|_{2,\Omega \times (0,T)} + \|v\|_{2,\Omega \times (0,T)} \leq L_T, \quad \text{and} \quad (u, v) = \lambda \mathcal{L}_R(u, v), \quad (19)$$

[see Schaefer's Theorem in [Evans \(1998\)](#)]. To this end, it can be shown that

$$\int_0^T ((u_t, \gamma) + (\nabla u, \nabla \gamma)) \, dt = \int_0^T \lambda (h_{1,R}(u_+, v_+), \gamma) \, dt, \quad (20a)$$

$$\int_0^T ((v_t, \gamma) + \delta(\nabla v, \nabla \gamma)) \, dt = \int_0^T \lambda (h_{2,R}(u_+, v_+), \gamma) \, dt, \quad (20b)$$

for all $\gamma \in W_{\text{per}}^{1,1}(\Omega \times (0, T))$. Choosing $\gamma = u_-$ in the first equation, $\gamma = v_-$ in the second equation, and observing that $u_- h_{1,R}(u_+, v_+), v_- h_{2,R}(u_+, v_+) \geq 0$, we can easily show that $u_-, v_- = 0$, implying $u = u_+$ and $v = v_+$. From this, it follows from the definitions for h_1 and h_2 that there exists $K > 0$, independent of u, v and R , so that $h_{i,R}(u, v) \leq K(u + v)$ for $i = 1, 2$. Now substitute $\gamma = u$ in Eq. (20a) and $\gamma = v$ in Eq. (20b). Then, the estimate above and Gronwall's inequality guarantee the estimate in (19). As a result, \mathcal{L}_R has a fixed point, and this fixed point can be shown to be a solution of Problem III provided we can obtain an L^∞ estimate for u and v independent of $R > 0$. This can be achieved by iteratively choosing $\gamma = u^k$ and $\gamma = v^k$ in (20a) and (20b) for successively larger values of $k \in \mathbb{N}$ and $\lambda = 1$ to obtain $L^p(\Omega \times (0, T))$ estimates for u and v independent of R and p . As a result, Problem III has a solution, and there is a uniform L^∞ estimate for the solution. (Note: If we work harder, we can prove that the estimate is also independent of $T > 0$.) This uniform estimate can be used, along with Gronwall's inequality to prove that Problem III has a unique global solution, and there is a function $\varphi \in C([0, \infty))$ such that $0 \leq u(\cdot, t), v(\cdot, t) \leq \varphi(t)$ for all $t \geq 0$. \square

3 Numerical Schemes

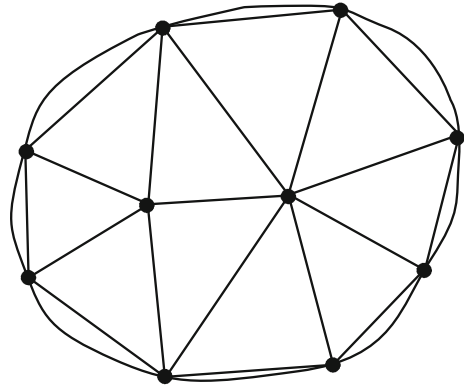
We approximate the predator–prey system (1) with initial conditions (2), and either the Robin–Neumann boundary conditions (9), the Dirichlet–Neumann boundary conditions (10), or the Periodic boundary conditions (8). The method involves applying the standard Galerkin finite element method for the spatial discretization, coupled with a (linear) semi-implicit time-stepping scheme for each boundary condition case.

3.1 Set-up of the Finite Element Method

For convenience, prior to stating the fully discrete approximations, we provide some preliminary results and set-up details. Initially, we discretize space and time and also replace the infinite dimensional function spaces by finite dimensional subspaces.

Let $\mathcal{T}^h = \{\tau\}$ be a partitioning of the domain Ω into approximately equilateral nonoverlapping closed triangles τ , h_τ denotes the length of the longest side of τ ,

Fig. 1 Domain Ω with triangulation



$h = \max h_\tau$ for all triangles τ in \mathcal{T}^h and $\Omega_h = \bigcup_{\tau \in \mathcal{T}^h} \bar{\tau}$ (illustrated in Fig. 1). Triangles must intersect along a common edge, at a common vertex, or not at all. We assume that the step size h is small enough so the error in approximating our problem over the domain Ω_h instead of Ω is negligible. Associated with \mathcal{T}^h is the finite dimensional subspace of $H^1(\Omega)$, consisting of piecewise linear continuous functions given by

$$S^h := \{w \in C(\Omega_h) : w \text{ is linear on each } \tau\}.$$

Let $\varphi_1, \varphi_2, \dots, \varphi_J$ be the basis functions for S^h satisfying $\varphi_j(\mathbf{x}_k) = \delta_{kj}$, where $\mathbf{x}_1, \mathbf{x}_2, \dots, \mathbf{x}_J$ are the nodes (triangle vertices) of \mathcal{T}^h and δ_{kj} is the Kronecker delta function.³ It follows that any $v \in S^h$ can be written as a linear combination of the basis functions weighted by the nodal values, i.e. $v(\mathbf{x}) = \sum_{i=1}^J v(\mathbf{x}_i)\varphi_i(\mathbf{x})$. We introduce the piecewise linear interpolation operator $I^h : C(\Omega_h) \mapsto S^h$ such that $I^h w(\mathbf{x}_k) = w(\mathbf{x}_k)$ for all $k = 1, \dots, J$. We shall also need a discrete L^2 inner product on $C(\Omega_h)$ defined by

$$(u, v)^h := \int_{\Omega} I^h(u(\mathbf{x})v(\mathbf{x})) \, d\mathbf{x} \equiv \sum_{k=1}^J \widehat{M}_{kk} u(\mathbf{x}_k)v(\mathbf{x}_k), \quad (21)$$

where $\widehat{M}_{ii} := (1, \varphi_i) \equiv \int_{\Omega} \varphi_i \, d\mathbf{x}$ corresponds to the diagonal ‘lumped mass matrix’ M . Observe using (21) that

$$(\varphi_i, \varphi_j)^h \equiv \widehat{M}_{jj} \delta_{ij}. \quad (22)$$

The ‘Vertex Quadrature’ rule (Ciarlet 1979) used in the evaluation of the above discrete L^2 inner product (21) is just the two-dimensional equivalent of the familiar Trapezoid rule for numerically integrating a continuous function in one space dimension. For later use, we also define the following matrices:

$$K_{ij} := \int_{\Omega} \nabla \varphi_i \cdot \nabla \varphi_j \, d\mathbf{x} \quad (\text{‘Stiffness Matrix’ } K), \quad (23a)$$

$$L_{ij} := (\widehat{M}_{ii})^{-1} K_{ij}, \quad (\text{‘Finite Element Matrix’ } L). \quad (23b)$$

³ A typical basis function is illustrated in many textbooks on the finite element method (e.g. Johnson (2009, p. 29)).

For further details concerning relevant background finite element theory, see [Barrett and Blowey \(1996\)](#), [Blowey and Elliott \(1992\)](#), [Garvie and Blowey \(2005\)](#), [Garvie and Trenchea \(2007\)](#), [Thomé \(2006\)](#), [Larsson and Thomée \(2009\)](#).

3.2 Fully Discrete Finite Element Methods

We uniformly subdivide the time interval $[0, T]$ with time levels $t_n = n\Delta t$, $n = 1, 2, \dots, N$, where the time step is $\Delta t := T/N$. In order to write down the fully discrete finite element method, we define the following time discretizations of the continuous reaction kinetics (12):

$$\widehat{h}_1(U^n, U^{n-1}, V^n) := U^n - U^n|U^{n-1}| - \frac{U^{n-1}V^n}{|U^{n-1}| + \alpha} \approx h_1(u, v), \tag{24a}$$

$$\widehat{h}_2(U^{n-1}, V^n) := \frac{\beta U^{n-1}V^n}{|U^{n-1}| + \alpha} - \gamma V^n \approx h_2(u, v), \tag{24b}$$

where the finite element solutions U^n and V^n approximate the continuous solutions u and v at time level t_n . Observe that the approximate reaction kinetics are linear with respect to the solutions at time level t_n , and if algebraically $U^n = U^{n-1} = u$ and $V^n = v$, then the approximate reaction kinetics reduce to their continuous counterparts. (The absolute values used in (24) make no difference to a correctly converged solution as they are nonnegative.)

The starting points for the finite element methods are the Weak Problems I, II, and III, given by (13), (14), and (16), respectively. In each case, we replace the continuous trial and test spaces with their finite dimensional approximations and discretize the variational formulations. This approach is called the ‘Galerkin method’ ([Grossmann et al. 2007](#), p. 152).

The finite element method corresponding to the Weak Problem I [see (13)] is given by (cf. [Garvie and Trenchea 2007](#)):

Finite Dimensional Weak Problem I: Given initial approximations $U^0 = I^h u_0$, $V^0 = I^h v_0$, for $n = 1, 2, \dots, N$ find $U^n, V^n \in S^h$ such that

$$\left(\frac{U^n - U^{n-1}}{\Delta t}, \chi\right)^h + (\nabla U^n, \nabla \chi) = k_1(U^{n-1}, \chi)_{\Gamma_1}^h + (g_u^n, \chi)_{\Gamma_2}^h + (\widehat{h}_1, \chi)^h, \tag{25a}$$

$\forall \chi \in S^h,$

$$\left(\frac{V^n - V^{n-1}}{\Delta t}, \chi\right)^h + \delta(\nabla V^n, \nabla \chi) = k_2(V^{n-1}, \chi)_{\Gamma_1}^h + (g_v^n, \chi)_{\Gamma_2}^h + (\widehat{h}_2, \chi)^h. \tag{25b}$$

$\forall \chi \in S^h,$

where $g_u^n := g_u|_{t=t_n}$ and $g_v^n := g_v|_{t=t_n}$. As the functions $\nabla U^n \cdot \nabla \chi$ and $\nabla V^n \cdot \nabla \chi$ are piecewise constant, there is no need to use the discrete L^2 inner product to evaluate

these terms as the Vertex Quadrature rule (21) is exact for piecewise polynomials of degree one or less.

Before we present the finite element method corresponding to the Weak Problem II, we define the following finite dimensional approximations of the trial and test spaces used in the infinite dimensional problem:

$$\begin{aligned} S_{E_u}^h &:= \{\chi \in S^h : \chi = f_u(\mathbf{x}, t) \text{ on } \Gamma_1\} \subset H_{E_u}^1(\Omega), \\ S_{E_v}^h &:= \{\chi \in S^h : \chi = f_v(\mathbf{x}, t) \text{ on } \Gamma_1\} \subset H_{E_v}^1(\Omega), \\ S_0^h &:= \{\chi \in S^h : \chi = 0 \text{ on } \Gamma_1\} \subset H_0^1(\Omega; \Gamma_1). \end{aligned}$$

The finite element method corresponding to the Weak Problem II [see (14)] is given by:

Finite Dimensional Weak Problem II: Given initial approximations $U^0 = I^h u_0$, $V^0 = I^h v_0$, for $n = 1, 2, \dots, N$ find $U^n \in S_{E_u}^h$, $V^n \in S_{E_v}^h$ such that

$$\left(\frac{U^n - U^{n-1}}{\Delta t}, \chi\right)^h + (\nabla U^n, \nabla \chi) = (g_u^n, \chi)_{\Gamma_2}^h + (\widehat{h}_1, \chi)^h, \quad \forall \chi \in S_0^h, \quad (26a)$$

$$\left(\frac{V^n - V^{n-1}}{\Delta t}, \chi\right)^h + \delta(\nabla V^n, \nabla \chi) = (g_v^n, \chi)_{\Gamma_2}^h + (\widehat{h}_2, \chi)^h, \quad \forall \chi \in S_0^h, \quad (26b)$$

where $g_u^n := g_u|_{t=t_n}$ and $g_v^n := g_v|_{t=t_n}$.

To present the finite element method corresponding to the Weak Problem III, we need the following finite dimensional approximation space:

$$S_{\text{per}}^h := \left\{ \chi \in S^h : \chi(a, y) = \chi(b, y), \chi(x, a) = \chi(x, b), \forall x, y \in [a, b] \right\}.$$

The finite element method corresponding to the Weak Problem III [see (16)] is then given by:

Finite Dimensional Weak Problem III: Given initial approximations $U^0 = I^h u_0$, $V^0 = I^h v_0$, for $n = 1, 2, \dots, N$ find $U^n, V^n \in S_{\text{per}}^h$ such that

$$\left(\frac{U^n - U^{n-1}}{\Delta t}, \chi\right)^h + (\nabla U^n, \nabla \chi) = (\widehat{h}_1, \chi)^h, \quad \forall \chi \in S_{\text{per}}^h, \quad (27a)$$

$$\left(\frac{V^n - V^{n-1}}{\Delta t}, \chi\right)^h + \delta(\nabla V^n, \nabla \chi) = (\widehat{h}_2, \chi)^h, \quad \forall \chi \in S_{\text{per}}^h. \quad (27b)$$

3.3 Derivation of the Linear Systems of Equations

The finite element methods are linear with respect to the solutions at the time level t_n ; thus, they can be re-written as systems of linear algebraic equations. First recall that the finite element solutions U^n and V^n belong to the finite dimensional subspace S^h ,

and thus, they can be written in the forms

$$U^n(\mathbf{x}) = \sum_{j=1}^J U_j^n \varphi_j(\mathbf{x}), \quad V^n(\mathbf{x}) = \sum_{j=1}^J V_j^n \varphi_j(\mathbf{x}),$$

where $U_j^n = U^n(\mathbf{x}_j)$ and $V_j^n = V^n(\mathbf{x}_j)$. We also take the test functions $\chi = \varphi_i$, for $i = 1, 2, \dots, J$. For notational convenience, we often suppress the dependence on \mathbf{x} .

We start by deriving the linear system of equations associated with the Finite Dimensional Weak Problem I, i.e. (25a)–(25b).

Using the above expansions for U^n and V^n , the specific choice for χ , (21), (22), (23a), and the definition of the lumped mass matrix yields

$$\frac{(U_i^n - U_i^{n-1})}{\Delta t} \widehat{M}_{ii} + \sum_{j=1}^J K_{ij} U_j^n = k_1 U_i^{n-1} (1, \varphi_i)_{\Gamma_1} + g_u(x_i, t_n) (1, \varphi_i)_{\Gamma_2} + \widehat{M}_{ii} \widehat{h}_1, \tag{28a}$$

$$\frac{(V_i^n - V_i^{n-1})}{\Delta t} \widehat{M}_{ii} + \delta \sum_{j=1}^J K_{ij} V_j^n = k_2 V_i^{n-1} (1, \varphi_i)_{\Gamma_1} + g_v(x_i, t_n) (1, \varphi_i)_{\Gamma_2} + \widehat{M}_{ii} \widehat{h}_2. \tag{28b}$$

Multiplying both equations by $\Delta t (\widehat{M}_{ii})^{-1}$, recalling (23b) and rearranging yields the following system of $2J$ linear algebraic equations for each time step:

Linear System I: For $n = 1, \dots, N$ solve

$$A_1^{n-1} U^n + \Delta t B_1^{n-1} V^n = U^{n-1} + \Phi_1^{n-1}, \tag{29a}$$

$$C_1^{n-1} V^n = V^{n-1} + \Psi_1^{n-1}, \tag{29b}$$

with

$$\begin{aligned} \{U^n\}_i &:= U_i^n, \quad \{V^n\}_i := V_i^n, \\ U_i^0 &= u_0(x_i), \quad V_i^0 = v_0(x_i), \\ A_1^{n-1} &:= (1 - \Delta t)I + \Delta t L + \mathfrak{D}_1^{n-1}, \\ B_1^{n-1} &:= \Delta t \mathfrak{D}_2^{n-1}, \\ C_1^{n-1} &:= (1 + \Delta t \gamma)I + \delta \Delta t L - \Delta t \beta \mathfrak{D}_2^{n-1}, \\ \mathfrak{D}_1^{n-1} &:= \text{diag}\{|U_1^{n-1}|, |U_2^{n-1}|, \dots, |U_J^{n-1}|\}, \\ \mathfrak{D}_2^{n-1} &:= \text{diag}\left\{\frac{U_1^{n-1}}{|U_1^{n-1}| + \alpha}, \frac{U_2^{n-1}}{|U_2^{n-1}| + \alpha}, \dots, \frac{U_J^{n-1}}{|U_J^{n-1}| + \alpha}\right\}, \\ \{\Phi_1^{n-1}\}_i &:= \Delta t (\widehat{M}_{ii})^{-1} \left(k_1 U_i^{n-1} (1, \varphi_i)_{\Gamma_1} + g_u(x_i, t_n) (1, \varphi_i)_{\Gamma_2}\right), \\ \{\Psi_1^{n-1}\}_i &:= \Delta t (\widehat{M}_{ii})^{-1} \left(k_2 V_i^{n-1} (1, \varphi_i)_{\Gamma_1} + g_v(x_i, t_n) (1, \varphi_i)_{\Gamma_2}\right). \end{aligned}$$

The derivation of the linear system of equations associated with the Finite Dimensional Weak Problem II, i.e. (26a)–(26b), is similar to the derivation of Linear System I, but with some important differences. In practice, the Dirichlet conditions are implemented by first formulating the pure Neumann problem, which generates a finite element equation for every node. The problem formulation is then modified, so every finite element equation corresponding to a node on Γ_1 is replaced by an equation enforcing the Dirichlet conditions directly into the resulting system of linear algebraic equations at each time step, which is described below.

Initially, in an analogous manner to the derivation of (28a)–(28b), the Finite Dimensional Weak Problem II leads to the linear system of equations, for $n = 1, \dots, N$

$$A_1^{n-1}U^n + \Delta t B_1^{n-1}V^n = \widehat{\text{rhs}}_u, \tag{30a}$$

$$C_1^{n-1}V^n = \widehat{\text{rhs}}_v, \tag{30b}$$

with

$$\widehat{\text{rhs}}_u := U^{n-1} + \widehat{\Phi}_1^{n-1}, \quad \text{where } \{\widehat{\Phi}_1^{n-1}\}_i := \Delta t (\widehat{M}_{ii})^{-1} g_u(x_i, t_n) (1, \varphi_i)_{\Gamma_2},$$

$$\widehat{\text{rhs}}_v := V^{n-1} + \widehat{\Psi}_1^{n-1}, \quad \text{where } \{\widehat{\Psi}_1^{n-1}\}_i := \Delta t (\widehat{M}_{ii})^{-1} g_v(x_i, t_n) (1, \varphi_i)_{\Gamma_2},$$

and the other terms are the same as in Linear System I. Now to incorporate the Dirichlet conditions $u = g_u$ and $v = g_v$ at node x_i on Γ_1 , we modify the i th equation of the linear system (30a) via

$${}^i \begin{pmatrix} 0 & \dots & 0 & 1 & 0 & \dots & 0 \end{pmatrix} \begin{pmatrix} U_i^n \end{pmatrix} + \Delta t \begin{pmatrix} 0 & \dots & 0 & \dots & 0 \end{pmatrix} \begin{pmatrix} V_i^n \end{pmatrix} = \begin{pmatrix} g_u^{i,n} \end{pmatrix},$$

where $g_u^{i,n} := g_u(x_i, t_n)$ and the i th equation of the linear system (30b) via,

$${}^i \begin{pmatrix} 0 & \dots & 0 & 1 & 0 & \dots & 0 \end{pmatrix} \begin{pmatrix} V_i^n \end{pmatrix} = \begin{pmatrix} g_v(x_i, t_n) \end{pmatrix},$$

where the entry ‘1’ is incorporated at the i th row and the i th column of the matrices A_1^{n-1} and C_1^{n-1} . The Dirichlet conditions are imposed for all nodes x_i on Γ_1 . The resulting modified linear system of $2J$ linear equations for each time step is expressed as follows:

Linear System II: For $n = 1, \dots, N$ solve

$$A_2^{n-1}U^n + \Delta t B_2^{n-1}V^n = \text{rhs}_u, \tag{31a}$$

$$C_2^{n-1}V^n = \text{rhs}_v, \tag{31b}$$

where A_2^{n-1} , B_2^{n-1} , C_2^{n-1} , $\widehat{\text{rhs}}_u$, and $\widehat{\text{rhs}}_v$ are the adjusted versions of A_1^{n-1} , B_1^{n-1} , C_1^{n-1} , $\widehat{\text{rhs}}_u$, and $\widehat{\text{rhs}}_v$, respectively, incorporating the Dirichlet boundary conditions.

The derivation of the linear system of equations associated with the Finite Dimensional Weak Problem III is similar to the derivation of Linear System II. In practice, the Periodic boundary conditions are implemented by first formulating the pure Neumann problem, which generates a finite element equation for every node. The problem formulation is then modified, so for each pair of nodes linked by a Periodic boundary condition, one finite element equation is replaced by an equation enforcing equality of values at the two nodes.

Initially, in an analogous manner to the derivation of (30a)–(30b), the Finite Dimensional Weak Problem III leads to the linear system of equations, for $n = 1, \dots, N$

$$A_1^{n-1}U^n + \Delta t B_1^{n-1}V^n = U^{n-1}, \tag{32a}$$

$$C_1^{n-1}V^n = V^{n-1}, \tag{32b}$$

where the coefficient matrices are the same as those in (29a)–(29b). Now to incorporate the Periodic boundary conditions, we label the sides of the square bn1, bn2, bn3, and bn4 such that $\Gamma := \text{bn1} \cup \text{bn2} \cup \text{bn3} \cup \text{bn4}$. Thus, the periodic conditions are given by

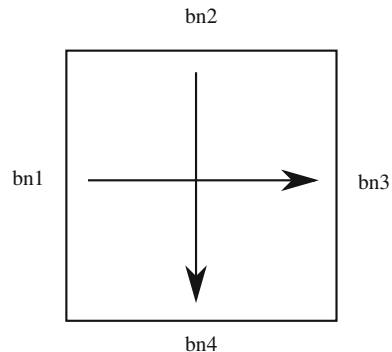
$$u|_{\text{bn3}} = u|_{\text{bn1}}, \quad v|_{\text{bn3}} = v|_{\text{bn1}}, \tag{33}$$

$$u|_{\text{bn4}} = u|_{\text{bn2}}, \quad v|_{\text{bn4}} = v|_{\text{bn2}}, \tag{34}$$

(see Fig. 2). For example, to prescribe U_i^n and V_i^n at the (‘target’) node x_i on bn3 to be equal to U_j^{n-1} and V_j^{n-1} at the (‘source’) node x_j on bn1, we modify the i th equations in (32) via

$$i \begin{pmatrix} 0 & \dots & 0 & 1 & 0 & \dots & 0 \end{pmatrix} \begin{pmatrix} U_i^n \end{pmatrix} + \Delta t \begin{pmatrix} 0 & \dots & 0 & \dots & 0 \end{pmatrix} \begin{pmatrix} V_i^n \end{pmatrix} = \begin{pmatrix} U_j^{n-1} \end{pmatrix},$$

Fig. 2 Imposing periodic boundary conditions on the square



3.4.2 Description of FE2DX_ND

The codes are function files, so to run the code one just types the name of the code (in lower case) at the MATLAB prompt. Prior to running the code, the user must construct the unstructured grid for the problem using a separate meshing program. There are many 2D meshing programs; however, we recommend MESH2D, freely available at <http://www.mathworks.com/matlabcentral/fileexchange/>, as it is a MATLAB program, and we have verified its effectiveness. The unstructured grid generation provides the triangle enumeration ('t_triang.dat') and the nodal coordinates ('p_coord.dat'), which are loaded by FE2DX_ND as external files. A simple example given at <http://www.uoguelph.ca/~mgarvie/> explains the required structure of these arrays. In addition, the code loads the external files 'bn1_nodes.dat' and 'bn2_nodes.dat', which are the node lists for Γ_1 and Γ_2 . An example of a simple 'front-end' written in MATLAB for identifying the node lists for a hypothetical lake problem with an island is given at the above-mentioned website.

Program FE2DX_ND is structured as follows:

- Lines 23–46: External data files for the mesh are loaded.
- Lines 50–78: User prompted for the parameter values, initial data functions, Dirichlet data functions, and Neumann data functions. The functions are entered as strings (allowable formats discussed below) and then converted to anonymous functions.
- Lines 82–140: The Stiffness Matrix K and the Finite Element Matrix L are assembled. As this is more involved an explanation for this part of the code is given in "Appendix".
- Lines 141–143: The constant coefficient parts of the matrices A_2 and C_2 in Linear System II are constructed.
- Lines 147–197: The Linear System II is solved repeatedly from t_1 to $t_N = T$.
 - Lines 149–157: The coefficient matrices A_2 , B_2 , and C_2 are updated with the current solutions, as is the right-hand side of Linear System II.
 - Lines 158–173: The Neumann boundary conditions are imposed for each edge of Γ_2 .
 - Lines 174–186: The Dirichlet boundary conditions are imposed for each node on Γ_1 .
 - Lines 187–189: The Incomplete LU factorizations of the coefficient matrices A_2 and C_2 are computed to provide preconditioners for the GMRES iterative solver.
 - Lines 190–196: Linear System II is solved using the GMRES iterative solver.
- Lines 201–214: The finite element solutions for u and v are plotted using a triangular surface plot at time T (a vertical 'colorbar' provides a scale).

There is no special way to enter the data functions. Unlike the simpler MATLAB codes presented by Garvie (2007), the element-by-element rules for expressing arithmetic operations are not required. An example of an acceptable input format for the boundary functions is the following:

```
>> Enter the Dirichlet b.c. glu(x,y,t) for u
0.2*sin(x^2-y^2)+t/10+0.2
>> Enter the Dirichlet b.c. glv(x,y,t) for v
0.3*cos(x^2-y^2)+t/20+0.3
>> Enter the Neumann b.c. g2v(x,y,t) for v 0.0
>> Enter the Neumann b.c. g2v(x,y,t) for v 0.6
```

This last two entries show we may enter a single number for a constant function. A similar format is used for entering the initial data, although the functions depend on space, but not time. For example:

```
>> Enter initial data function u0(x,y) 0.2*exp(-(x^2+y^2))
>> Enter initial predator function v0(x,y) 1.0
```

We can also define functions in a piecewise fashion. For example, with $\Omega = [0, 100]^2$, to choose an initial predator density of 0.2 within a circle with radius 5 units and centre (50, 50), and a density of 0 elsewhere on Ω , we input the following:

```
>> Enter initial data function u0(x,y) 0.2*((x-50)^2+(y-50)^2<25)
```

It is also possible to enter piecewise-defined functions utilizing MATLAB's logical (scalar) operators && ('AND'), || ('OR'), ~ ('NOT').

4 Numerical Experiments

We present the results of nine numerical experiments, which were motivated by discussions and experiments in the literature. In each case, we give sufficient details so the results of the experiments can be reproduced using our MATLAB codes, or repeated using different numerical methods. This is advantageous as it allows theoretical biologists to verify our results and use the findings as a starting point for further study.

The finite element methods were coded in MATLAB (ver R2013b). The resulting sparse linear systems were solved with the aid of MATLAB's intrinsic GMRES (Generalized Minimum Residual Method) function, preconditioned with the intrinsic ILU (Incomplete LU factorization) function. As the discrete problem may admit spurious solutions (Garvie 2007) and analytical solutions of the continuous problem are not known, extra efforts were taken to verify convergence. In addition to using mesh refinement and time step reduction to check convergence, solutions were also independently verified by computing the solutions in COMSOL (ver 4.4), which employs higher-order solvers in both space and time. Furthermore, we computed the solutions using the generalizations of 'Scheme 1' (described in Sect. 3.2) and 'Scheme 2' (Garvie 2007) and verified that solutions were virtually identical for both schemes. In all cases, the geometry and unstructured grids were generated in COMSOL and then exported to MATLAB using LiveLink for MATLAB prior to solution. This facilitated the comparison of numerical results in MATLAB and COMSOL.⁴ Solutions were

⁴ The unstructured grids can be generated using any other suitable meshing software, for example, MESH2D available at <http://www.mathworks.com/matlabcentral/fileexchange/>.

Table 1 Parameter values used in the numerical Experiments 1–9

| | 1 | 2 | 3 | 4 | 5 | 6 | 7 | 8 | 9 |
|---------------|---------|---------|--------|--------|--------|--------|---------|--------|--------|
| α | 0.4 | 0.4 | 0.2 | 0.204 | 0.4 | 0.4 | 0.4 | 0.4 | 0.2 |
| β | 2 | 2 | 1 | 0.83 | 2 | 2 | 2 | 2 | 1 |
| γ | 0.6 | 0.6 | 0.5 | 0.46 | 0.6 | 0.6 | 0.6 | 0.6 | 0.5 |
| δ | 1 | 1 | 1 | 1 | 1 | 10 | 1 | 1 | 5 |
| h_{\max} | 2 | 2 | 2 | 2 | 2 | 2 | 1 | 1 | 2 |
| h_{\min} | 3.46E−4 | 3.46E−4 | 0.0605 | 0.0321 | 0.03 | 0.197 | 1 | 0.03 | 0.15 |
| T | 150 | 150 | 200 | 94 | 39 | 90 | 1000 | 300 | 100 |
| no_e | 100,184 | 70,914 | 56,215 | 45,082 | 24,830 | 95,824 | 420,668 | 24,809 | 50,818 |
| n | 50,493 | 36,162 | 28,440 | 23,934 | 12,574 | 48,595 | 211,135 | 12,564 | 25,767 |

We denote h_{\max} and h_{\min} to be the maximum and minimum element sizes for the meshes, no_e the number of elements in each mesh, and n denotes the number of nodes in the mesh. The stationary values u^* and v^* are calculated from (3). The meaning of the other parameters is given in the text

run on a Mac Pro with a 3.5 GHz 6-Core Intel Xeon E5 processor and 32 GB of memory. Simulations took between 20 minutes and a day to run, depending on the experiment. The parameter values for each experiment are shown in Table 1. A time step of $\Delta t = 1/384$ was used for all numerical simulations as this was found to be sufficient to obtain convergence, except for the solutions in Experiment 7 (see below). The domain geometry, initial data, and boundary conditions are described below.

Experiment 1 For our first experiment, we used the finite element code FE2DX_N_FAST to approximate the predator–prey system (1) over the square domain $\Omega := [0, 400]^2$, with homogeneous Neumann boundary conditions. The initial data were prescribed as (see Medvinsky et al. 2002; Garvie 2007; Garvie and Trenchea 2007)

$$u_0(x, y) := u^* - 2 \times 10^{-7}(x - 0.1y - 225)(x - 0.1y - 675), \tag{36a}$$

$$v_0(x, y) := v^* - 3 \times 10^{-5}(x - 450) - 1.2 \times 10^{-4}(y - 150), \tag{36b}$$

which rapidly led to the formation of rotating spiral waves (see Fig. 3a).

Experiment 2 In the second experiment, we repeated Experiment 1, again using FE2DX_N_FAST, but replaced the square domain with the geometry of a Koch Snowflake (Falconer 1990) (node list available from <http://www.uoguelph.ca/~mgarvie/>). The results were qualitatively similar to those obtained in Experiment 1 (see Fig. 3b).

Experiment 3 In the third experiment, we used FE2DX_ND_FAST to approximate the predator–prey system over an irregular domain containing an obstacle. Homogeneous Dirichlet boundary conditions (for both predators and prey) were imposed on the outer boundary of the domain and homogeneous Neumann boundary conditions on the edge of the obstacle (node lists available from <http://www.uoguelph.ca/~mgarvie/>). Starting from stationary initial data (u^*, v^*), this scenario led to the generation of periodic

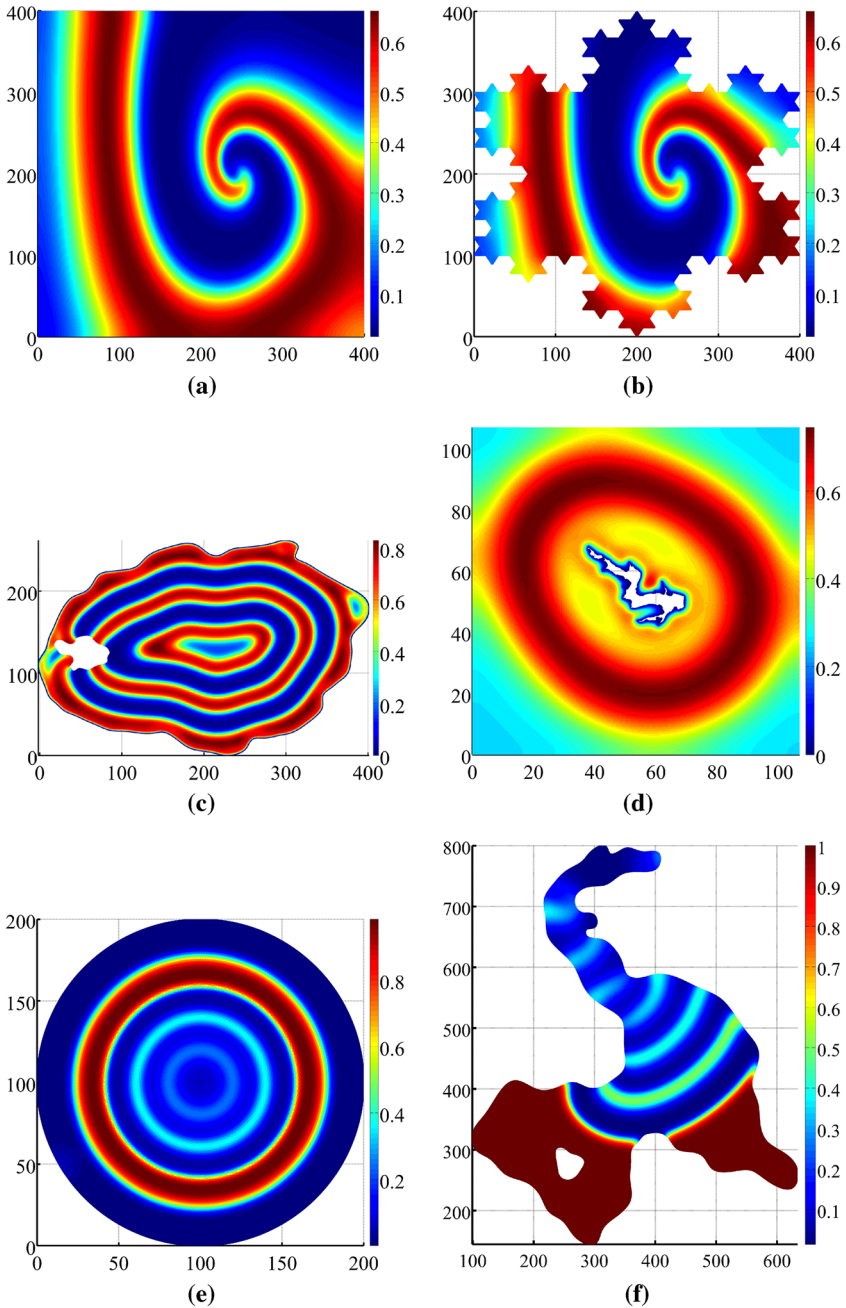


Fig. 3 (Color figure line) 2D numerical solutions of the predator–prey system (1): **a** snapshot of prey density for Experiment 1 at $T = 150$; **b** snapshot of prey density for Experiment 2 at $T = 150$; **c** snapshot of prey density for Experiment 3 at $T = 200$; **d** snapshot of prey density for Experiment 4 at $T = 94$; **e** snapshot of prey density for Experiment 5 at $T = 39$; **f** snapshot of prey density for Experiment 6 at $T = 90$. For the initial conditions, boundary conditions, and parameters used see the text and Table 1

travelling waves ('target waves'), which are similar to the results displayed in Figure 10 of Sherratt (2003). The wave front moves from the outer edge of the domain towards the centre of the domain; however, the periodic travelling waves move in the opposite direction (see Fig. 3c).

Experiment 4 In the fourth experiment, we used FE2DX_ND_FAST to approximate the predator–prey system over a square domain $[0, 107]^2$ enclosing an irregular obstacle, based on the scanned image of a reservoir (Kielder Water, UK) in a forest (the node list for the geometry of the obstacle is available from <http://www.uoguelph.ca/~mgarvie/>). To model a hostile boundary for the obstacle⁵, we imposed homogeneous Dirichlet boundary conditions on the edge of the obstacle and homogeneous Neumann boundary conditions on the sides of the square. Starting from stationary initial data (u^*, v^*) , target waves are generated by the obstacle, which are qualitatively similar to the results in Sherratt and Smith (2008), Yun et al. (2011) (see Fig. 3d).

Experiment 5 In the fifth experiment, we used FE2DX_N_FAST to approximate the predator–prey system over the circle, with radius 100 units, centre (100, 100), using homogeneous Neumann boundary conditions. The initial conditions correspond to colonization at the centre of an empty domain by predators and prey, given by

$$w_0(x, y) = \begin{cases} w^* & \text{if } (x - 100)^2 + (y - 100)^2 < 25, \\ 0 & \text{if } (x - 100)^2 + (y - 100)^2 \geq 25, \end{cases}$$

with w equal to u or v . With these initial conditions, the solutions rapidly evolve into expanding ring-like waves, followed by a succession of rings with smaller amplitudes (see Fig. 3e). The results of this experiment are qualitatively similar to the results of an analogous numerical experiment for a reaction–diffusion–advection system with ecological interactions of the Lotka–Volterra type (Dubois 1975). See also the discussion by Holmes et al. (1994, p. 22) regarding this situation.

Experiment 6 In the sixth experiment, we used FE2DX_N_FAST to approximate the predator–prey system in a fictitious 'lake' domain with an 'island' (the lists of nodes for the 'lake' and 'island' are available from <http://www.uoguelph.ca/~mgarvie/>). Homogeneous Neumann boundary conditions are imposed on both the 'lake' edge and the edge of the 'island'. The initial conditions are a small localized introduction of predators at the top of the domain, which is in the (stationary) prey only state, given by

$$v_0(x, y) = \begin{cases} v^* & \text{if } (x - 305)^2 + (y - 763)^2 < 100, \\ 0 & \text{if } (x - 305)^2 + (y - 763)^2 \geq 100, \end{cases}$$

$$u_0(x, y) = u^* \quad \text{everywhere.}$$

The solution evolved into regular periodic waves behind an invasive front, which rapidly moved from the initial point of introduction throughout the domain (see Fig. 3f).

⁵ See the paper by Sherratt and Smith (2008) for a biological motivation.

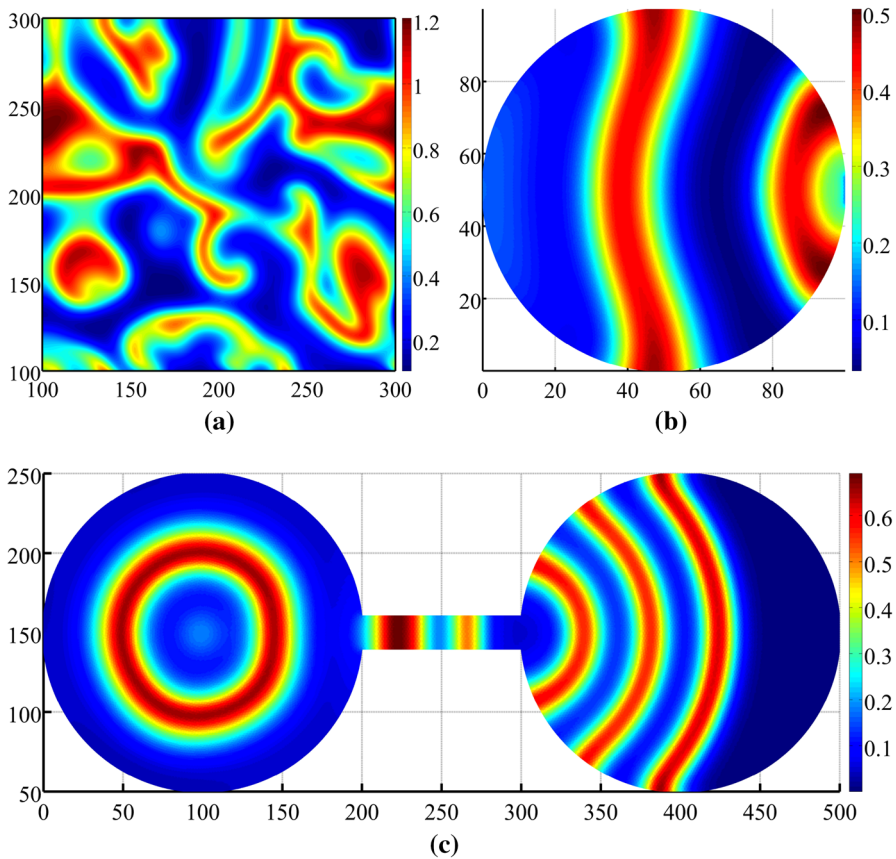


Fig. 4 (Color figure line) 2D numerical solutions of the predator–prey system (1): **a** snapshot of predator density for Experiment 7 at $T = 1,000$; **b** snapshot of prey density for Experiment 8 at $T = 300$; **c** snapshot of predator density for Experiment 9 at $T = 100$. For the initial conditions, boundary conditions, and parameters used, see the text and Table 1

The results and the experiment are similar to those performed by [Sherratt et al. \(1997\)](#) for a related spatially extended predator–prey system in two space dimensions. See also the discussion by [Holmes et al. \(1994, p. 22\)](#) regarding predator–prey interactions initiated in this manner.

Experiment 7 In the seventh experiment, we used `FE2DX_P_FAST` to approximate the predator–prey system in a square domain $[100, 300]^2$ with Periodic boundary conditions. The initial conditions are the same as the ones used in Experiment 1, but the problem is solved until a much larger final time T (see Table 1). The generation of spiral waves eventually breaks-up into what is termed in the literature ‘spatiotemporal chaos’ ([Medvinsky et al. 2002](#)) (see Fig. 4a). With a time step of $1/384$, we were unable to get an exact agreement with the results from `FE2D_P_FAST`, due to the chaotic nature of the solutions. The results of this experiment are qualitatively similar to those obtained if we replace the Periodic boundary conditions with homogeneous

Neumann boundary conditions [see Figure 5 in (Garvie 2007)]. Similar experiments were performed for a deterministic and stochastic phytoplankton–zooplankton system (a reaction–diffusion system with the Rosenzweig–MacArthur form) using Periodic boundary conditions (Malchow et al. 2004; Hilker et al. 2006).

Experiment 8 In the eighth experiment, we used FE2DX_NR_FAST to approximate the predator–prey system over the circle, with radius 50 units and centre (50, 50). We imposed mixed Robin–Neumann boundary conditions on the circumference of the circle. Specifically, in polar coordinates, with

$$\Gamma_1 := \{(r, \theta) : r = 50, \quad -5^\circ \leq \theta \leq 5^\circ\}, \quad \Gamma_2 := \{(r, \theta) : r = 50, \quad 5^\circ \leq \theta \leq 355^\circ\},$$

we imposed Neumann boundary conditions on Γ_2 and Robin boundary conditions on Γ_1 using $k_1 = k_2 = -0.5$. As k_1 and k_2 are negative, the Robin boundary conditions correspond to predators and prey leaving the domain via Γ_1 . Starting from the stationary initial data (u^* , v^*), this scenario led to the generation of periodic travelling waves moving away from Γ_1 and crossing the entire domain (see Fig. 4b). We were unable to find any comparable experiments in the literature for this experiment.

Experiment 9 In the ninth experiment, we used FE2DX_N_FAST to approximate the predator–prey system over a domain for metapopulation dynamics, using homogeneous Neumann boundary conditions and piecewise-defined initial data. The domain consists of two circles connected by a rectangular corridor. The first circle Ω_1 has radius 100 units and centre (100, 150). The second circle Ω_2 has radius 100 units and centre (400, 150). The corridor is given by the rectangle $\Omega_3 := [100 + 30\sqrt{11}, 400 - 30\sqrt{11}] \times [140, 160]$. The combined domain is given by $\Omega := \Omega_1 \cup \Omega_2 \cup \Omega_3$. To simulate the local extinction of predators in Ω_2 , we initially choose steady-state solutions for the predators and prey in Ω_1 , steady-state prey data in Ω_2 , and zero initial population density in the corridor Ω_3 , i.e.

$$u_0(x, y) = \begin{cases} u^* & \text{if } (x, y) \in \Omega \setminus \Omega_3 \\ 0 & \text{if } (x, y) \in \Omega_3 \end{cases}, \quad v_0(x, y) = \begin{cases} v^* & \text{if } (x, y) \in \Omega_1 \\ 0 & \text{if } (x, y) \in \Omega \setminus \Omega_1 \end{cases}.$$

The initial data evolved into periodic travelling waves for the predators, which passed through the corridor and re-populated the domain Ω_2 (see Fig. 4c). This experiment was motivated by a similar experiment conducted by Garvie et al. (2014) with a more sophisticated metapopulation model.

5 Discussion and Conclusions

5.1 Numerical Comments

One of the advantages of the MATLAB code is that once the external data for the mesh is supplied (boundary nodes, node, and triangle enumeration), then the approximation of the predator–prey system on a complicated domain with various boundary conditions

is as easy as the solution of the simpler problem on a square domain with standard boundary conditions. Of course, some initial efforts have to be made to set up the geometry, grid the domain, and post-process the mesh to identify node lists (possibly on different parts of the boundary).

Although we used the finite element method with piecewise linear continuous basis functions, quadratic or higher-order basis functions might yield a more accurate approximation. However, the method with linear basis functions is relatively simple and is supported by a rigorous numerical analysis by [Garvie and Trenchea \(2007\)](#). Furthermore, the finite element method yielded accurate solutions in all of the numerical experiments, except in Experiment 7, where we unable to obtain an adequate match between the two finite element methods due to the chaotic solutions.

The finite element method for the simpler problem studied over a square domain with homogeneous Neumann boundary conditions is only first-order accurate (in time) ([Garvie and Trenchea 2007](#)). Thus, the effective approximation of asymptotic solutions, or solutions displaying spatiotemporal chaos, may require more accurate numerical methods, for example, the Crank–Nicolson scheme ([Crank and Nicolson 1947](#)). A method showing promise for these types of problems is a finite element methods based on the composition of Implicit-Symplectic Euler steps (IMSP schemes) developed by [Diele et al. \(2014\)](#). The authors were able to reproduce some solutions by [Garvie \(2007\)](#) using considerably smaller time steps.

As theoretical biologists continue to model more complex problems, there will be a greater need for effective and user-friendly numerical methods.

5.2 Ecological Comments

The numerical experiments led to some general observations. The choice of domain shape, boundary conditions, and initial conditions has a crucial role to play in determining the spatiotemporal dynamics of solutions. The specific choice should reflect the particular ecological situation we wish to model. For example, the results of Experiments 1 and 2 show (at least for the transient solutions) that the shape of the boundary has little effect on the solutions when using homogeneous Neumann boundary conditions. Homogeneous Neumann boundary conditions may be adequate for modelling plankton dynamics in the ocean with an effectively unbounded domain. However, if the plankton lives in a lake with a lethal shoreline, then the appropriate boundary conditions are the homogeneous Dirichlet boundary conditions, and in this case, we expect the boundary to have a profound effect on the population dynamics (see Experiment 3).

The typical solutions for the predator–prey system (1) are periodic travelling waves in two space dimensions, which are either spiral waves, target waves, or waves of invasion. If these solution forms are unstable as solutions of the reaction–diffusion systems, then these solutions eventually break-up into spatiotemporal chaos (see Experiment 8). The paper by [Sherratt and Smith \(2008\)](#) reviews periodic travelling waves in cyclic populations and discusses the major mathematical research challenges in this area. A fundamental question raised that is particularly relevant to our paper is as follows: *What are the ecologically relevant mechanisms governing periodic travelling waves in natural populations?* As we have demonstrated, this question is easily investigated

by simulating different scenarios on a computer with the numerical methods presented in this paper. The results of our numerical experiments suggest that periodic travelling waves, or wave-like phenomena, can be caused by spatial heterogeneity in the model (see the discussion by [Sherratt and Smith \(2008\)](#)). Examples include: boundary conditions (Experiments 3 and 8); obstacles (Experiment 4); invasion (Experiments 5 and 6); and metapopulation dynamics (Experiment 9).

There are numerous problems requiring further investigation. For example, in Experiment 4, we could investigate the question: *How do the solutions change if we replace the Dirichlet boundary conditions with the more realistic Robin boundary conditions?* Another question we could easily investigate with the set-up of Experiments 5 or 6 is: *What happens when different waves of invasion meet?* In the context of metapopulation dynamics (see Experiment 9), a fundamental question is: *Do the long-term dynamics become asynchronous or synchronous?*⁶ This is important because it is believed asynchronous dynamics lead to the increased persistence of metapopulations ([Jansen 2001](#)).

The results and discussions in this paper highlight the need for researchers to investigate (both theoretically and numerically) more realistic ecological problems and the tools for doing so numerically are readily available.

Acknowledgments We are thankful for the comments of the handling editor and an anonymous reviewer that improved the accuracy and clarity of the paper. The research of M. Garvie was supported by a Natural Sciences and Engineering Research Council of Canada (NSERC) Discovery Grant #400159 and the research of J. Morgan was supported by a National Science Foundation (NSF) Grant DMS-0714864.

Appendix: Assembly of the Matrix K and L

Consider a generic triangle τ with nodes labelled P_i , P_j , and P_k , with coordinates (x_i, y_i) , (x_j, y_j) and (x_k, y_k) , respectively. Then, the linear basis function associated with node P_k can be expressed as⁷

$$\varphi_k(x, y) := \frac{h_{ji}(x, y)}{h_{ji}(x_k, y_k)}, \quad \text{where } h_{ji}(x, y) := (x - x_i)(y_j - y_i) - (x_j - x_i)(y - y_i),$$

($h_{ji}(x_k, y_k) \neq 0$), and the basis functions for the other nodes are defined analogously. Now as the gradient of the basis functions are constant on each triangle τ , all contributions to the Stiffness matrix K have the form $\int_{\tau} \nabla \varphi_s \cdot \nabla \varphi_p \, d\mathbf{x} = \nabla \varphi_s \cdot \nabla \varphi_p |\tau|$, where the area of the triangle τ is given by $|\tau| = |x_j y_k - x_k y_j - x_i y_k + x_k y_i + x_i y_j - x_j y_i|/2$. Elementary calculations yield

$$\nabla \varphi_k \cdot \nabla \varphi_i = \frac{(y_j - y_i)(y_k - y_j) + (x_i - x_j)(x_j - x_k)}{h_{ji}(x_k, y_k)h_{kj}(x_i, y_i)},$$

⁶ If the metapopulation dynamics are synchronous, then the dynamics in different patches are the same.

⁷ The full working for the assembly of these matrices was set as part of a project for a graduate course in Numerical Analysis ('Math*6400') at the University of Guelph, ON, Canada.

with similar expressions obtained for $\nabla\varphi_k \cdot \nabla\varphi_j$, $\nabla\varphi_i \cdot \nabla\varphi_j$, $|\nabla\varphi_k|^2$, $|\nabla\varphi_i|^2$ and $|\nabla\varphi_j|^2$. The contributions to the matrix $L := \bar{M}^{-1}K$ are readily calculated after noting $\int_{\tau} \varphi_i \, dx = \frac{1}{3}|\tau|$, where we used the fact that the volume of a tetrahedron is a third of the base area times the height.

References

- Adams R (1975) Sobolev spaces. Pure and applied mathematics. Academic Press, New York
- Ahmed M, Fiedler L (2002) A comparison of four rodent control methods in Philippine experimental rice fields. *Int Biodeterior Biodegrad* 49(2–3):125–132
- Alberty J, Carstensen C, Funken S (1999) Remarks around 50 lines of Matlab: short finite element implementation. *Numer Algorithms* 20(2–3):117–137
- Barrett J, Blowey J (1996) An error bound for the finite element approximation of a model for phase separation of a multi-component alloy. *IMA J Numer Anal* 16(2):257–287
- Barrett J, Elliott C (1986) Finite element approximation of the Dirichlet problem using the boundary penalty method. *Numer Math* 49:343–366
- Bassiri E, Bryant R, George M, Yerion K (2009) A finite difference method for modeling the formation of animal coat patterns. *Nonlinear Anal Real World Appl* 10(3):1730–1737
- Bittihn P, Squires A, Luther G, Bodenschatz E, Krinsky V, Parltitz U, Luther S (2010) Phase-resolved analysis of the susceptibility of pinned spiral waves to far-field pacing in a two-dimensional model of excitable media. *Phil Trans R Soc A* 368:2221–2236
- Blowey J, Elliott C (1992) The Cahn–Hilliard gradient theory for phase separation with nonsmooth free energy. Part II. Numerical analysis. *Eur J Appl Math* 3(2):147–179
- Brenner S, Scott L (1994) The mathematical theory of finite element methods. Vol. 15 of texts in applied mathematics. Springer, New York
- Cantrell R, Cosner C (2003) Spatial ecology via reaction–diffusion equations. Wiley series in mathematical and computational biology. Wiley, Chichester
- Cantrell R, Cosner C, Fagan W (1998) Competitive reversals inside ecological reserves: the role of external habitat degradation. *J Math Biol* 37:491–533
- Chaplain M, Ganesh M, Graham I (2001) Spatio-temporal pattern formation on spherical surfaces: numerical simulation and application to solid tumour growth. *J Math Biol* 42:387–423
- Ciarlet P (1979) The finite element method for elliptic problems. Vol. 4 of studies in mathematics and its applications. North-Holland, Amsterdam
- Crank N, Nicolson P (1947) A practical method for numerical evaluation of solutions of partial differential equations of the heat conduction type. *Proc Camb Phil Soc* 43:50–67
- Dawes J, Souza M (2013) A derivation of Hollings type I, II and III functional responses in predator–prey systems. *J Theor Biol* 327:11–22
- Descalzi O, Brand H (2008) Influence of boundary conditions on localized solutions of the cubic–quintic complex Ginzburg–Landau equation. *Prog Theor Phys* 119(5):725–738
- Diele F, Marangi C, Ragni S (2014) IMSP schemes for spatially explicit models of cyclic populations and metapopulation dynamics. *Math Comput Simul* 100:41–53
- Ding Y, Kawahara M (1998) Analysis of dynamic response of prey–predator system with nonlinear diffusion–reaction equations by using superposition. *Comput Methods Appl Mech Eng* 156:375–388
- Dubois D (1975) A model of patchiness for prey–predator plankton populations. *Ecol Model* 1:67–80
- Edelstein-Keshet L (2005) Mathematical models in biology. Vol. 46 of classics in applied mathematics. Society for Industrial and Applied Mathematics (SIAM), Philadelphia
- Evans L (1998) Partial differential equations. American Mathematical Society, Providence
- Fagan W, Cantrell R, Cosner C (1999) How habitat edges change species interaction. *Am Nat* 153(2):165–182
- Falconer K (1990) Fractal geometry. Wiley, Chichester
- Friedman A (2012) PDE problems arising in mathematical biology. *Netw Heterog Media* 7(4):691–703
- Garvie M (2007) Finite difference schemes for reaction–diffusion equations modelling predator–prey interactions in MATLAB. *Bull Math Biol* 69(3):931–956
- Garvie M, Blowey J (2005) A reaction–diffusion system of $\lambda - \omega$ type. Part II: numerical analysis. *Eur J Appl Math* 16(5):621–646

- Garvie M, Trenchea C (2007) Finite element approximation of spatially extended predator–prey interactions with the Holling type II functional response. *Numer Math* 107:641–667
- Garvie M, Trenchea C (2010) Spatiotemporal dynamics of two generic predator–prey models. *J Biol Dyn* 4(6):559–570
- Garvie M, Morgan J, Sharma V, (2014) A fully spatially structured metapopulation model for predator–prey dynamics in $d \leq 3$ space dimensions. (submitted)
- Grossmann C, Roos H-G, Stynes M (2007) Numerical treatment of partial differential equations. Springer, Berlin
- Gurney W, Veitch A, Cruickshank I, McGeachin G (1998) Circles and spirals: population persistence in a spatially explicit predator–prey model. *Ecology* 79(7):2516–2530
- Hilker F, Malchow H, Langlais M, Petrovskii S (2006) Oscillations and waves in a virally infected plankton system part II: transition from lysogeny to lysis. *Ecol Complex* 3:200–208
- Holden A, Markus M, Othmer H (eds) (1991) Nonlinear wave processes in excitable media. Plenum, New York
- Holling C (1959) Some characteristics of simple types of predation and parasitism. *Can Entomol* 91:385–398
- Holmes E, Lewis M, Banks J, Veit R (1994) Partial differential equations in ecology: spatial interactions and population dynamics. *Ecology* 75(1):17–29
- Jansen V (2001) The dynamics of two diffusively coupled predator–prey populations. *Theor Popul Ecol* 59:119–131
- Johnson C (2009) Numerical solution of partial differential equations by the finite element method. Dover, Mineola
- Kaipio J, Tervo J, Vauhkonen M (1995) Simulations of the heterogeneity of environments by finite elements. *Math Comput Simul* 39:155–172
- Ladyženskaja O, Solonikov V, Ural'ceva N (1968) Linear and quasilinear equations of parabolic type. Vol. 23 of translations of mathematical monographs. American Mathematical Society, Providence
- Larsson S, Thomée V (2009) Partial differential equations with numerical methods. Vol. 45 of texts in applied mathematics. Springer, Berlin
- Leung A (1982) A semilinear reaction–diffusion prey–predator system with nonlinear coupled boundary conditions: equilibrium and stability. *Indiana Univ Math J* 31(2):223–241
- Maciel G, Lutscher F (2013) How individual movement response to habitat edges affects population persistence and spatial spread. *Am Nat* 182(1):42–52
- Malchow H, Petrovskii S (2002) Dynamical stabilization of an unstable equilibrium in chemical and biological systems. *Math Comput Model* 36:307–319
- Malchow H, Radtke B, Kallache M, Medvinsky A, Tikhonov D, Petrovskii S (2000) Spatio-temporal pattern formation in coupled models of plankton dynamics and fish school motion. *Nonlinear Anal-Real* 1:53–67
- Malchow H, Petrovskii S, Medvinsky A (2002) Numerical study of plankton–fish dynamics in a spatially structured and noisy environment. *Ecol Model* 149:247–255
- Malchow H, Hilker F, Petrovskii S, Brauer K (2004) Oscillations and waves in a virally infected plankton system part I: the lysogenic stage. *Ecol Complex* 1:211–223
- Malchow H, Petrovskii S, Venturino E (2008) Spatiotemporal patterns in ecology and epidemiology: theory, models, and simulation. Vol. 17 of mathematical & computational biology. Chapman & Hall/CRC, Boca Raton
- Malpas L, Kennerley R, Hirons G, Sheldon R, Ausden M, Gilbert J, Smart J (2013) The use of predator-exclusion fencing as a management tool improves the breeding success of waders on lowland wet grassland. *J Nat Conserv* 21:37–47
- May R (1974) Stability and complexity in model ecosystems. Princeton University Press, New Jersey
- Medvinsky A, Petrovskii S, Tikhonova I, Malchow H, Li B-L (2002) Spatiotemporal complexity of plankton and fish dynamics. *SIAM Rev* 44(3):311–370
- Meinhardt H (1982) Models of biological pattern formation. Academic Press, New York
- Murray J (1981) On pattern formation mechanisms for lepidopteran wing patterns and mammalian coat markings. *Phil Trans R Soc Lond B* 295:473–496
- Murray J (2002) Mathematical biology I: an introduction, 3rd edition. Vol. 17 of interdisciplinary applied mathematics. Springer, New York
- Murray J (2003) Mathematical biology II: spatial models and biomedical applications, 3rd edition. Vol. 18 of interdisciplinary applied mathematics. Springer, New York
- Pascual M (1993) Diffusion-induced chaos in a spatial predator–prey system. *Proc R Soc Lond B* 251:1–7

- Peacock-Lopez E (2011) The relevance of cross-diffusion in the formation of Turing patterns. *Nonlinear Dyn Psychol Life Sci* 15(1):1–10
- Segel L, Jackson J (1972) Dissipative structure: an explanation and an ecological example. *J Theor Biol* 37:545–559
- Shangerganesh L, Balachandran K (2011) Existence and uniqueness of solutions of predator–prey type model with mixed boundary conditions. *Acta Appl Math* 116:71–86
- Sherratt J (2001) Periodic travelling waves in cyclic predator–prey systems. *Ecol Lett* 4:30–37
- Sherratt J (2003) Periodic travelling wave selection by Dirichlet boundary conditions in oscillatory reaction–diffusion systems. *SIAM J Appl Math* 63(5):1520–1538
- Sherratt J (2008) A comparison of periodic travelling wave generation by Robin and Dirichlet boundary conditions in oscillatory reaction–diffusion equations. *IMA J Appl Math* 73(5):759–781
- Sherratt J, Smith M (2008) Periodic travelling waves in cyclic populations: field studies and reaction–diffusion models. *J R Soc Interface* 5:483–505
- Sherratt J, Eagan B, Lewis M (1997) Oscillations and chaos behind predator–prey invasion: mathematical artifact or ecological reality? *Phil Trans R Soc Lond B* 352:21–38
- Sherratt J, Lambin X, Thomas C, Sherratt T (2002) Generation of periodic waves by landscape features in cyclic predator–prey systems. *Proc R Soc Lond B* 269:327–334
- Sherratt J, Lambin X, Sherratt T (2003) The effects of the size and shape of landscape features on the formation of travelling waves in cyclic populations. *Am Nat* 162:503–513
- Smith M, Sherratt J, Armstrong N (2008) The effects of obstacle size on periodic travelling waves in oscillatory reaction–diffusion equations. *Proc R Soc A* 464:365–390
- Smith M, Rademacher J, Sherratt J (2009) Absolute stability of wavetrains can explain spatiotemporal dynamics in reaction–diffusion systems of Lambda–Omega type. *SIAM J Appl Dyn Syst* 8(3):1136–1159
- Smoller J (1983) Shock waves and reaction–diffusion equations. Vol. 258 of *Grundlehren der mathematischen Wissenschaften*. Springer, New York
- Strang G, Fix G (1973) An analysis of the finite element method. Prentice-Hall, Englewood Cliffs
- Temam R (1997) Infinite-dimensional dynamical systems in mechanics and physics. Vol. 68 of *applied mathematical sciences*. Springer, New York
- Thomé V (2006) Galerkin finite element methods for parabolic problems, 2nd ed. Vol. 25 of *Springer series in computational mathematics*. Springer, Berlin
- Tilman D, Kareiva P (1997) Spatial ecology: the role of space in population dynamics and interspecific interactions. Vol. 30 of *monographs in population biology*. Princeton University Press, Princeton
- Yun A, Shin J, Li Y, Kim J (2011) Numerical study of periodic travelling wave solutions for the predator–prey model with landscape features. (submitted)